

Intermacromolecular complexes due to specific interactions. 12. Graft-like hydrogen bonding complexes based on pyridyl-containing polymers and end-functionalized polystyrene oligomers

Shiyong Liu, Quanming Pan, Jingwei Xie, Ming Jiang*

Institute of Macromolecular Science and Laboratory of Molecular Engineering of Polymers, Fudan University, Shanghai 200433, People's Republic of China

Received 9 September 1999; received in revised form 9 November 1999; accepted 19 November 1999

Abstract

Soluble graft-like complexes were obtained via hydrogen bonding interaction between poly(4-vinyl pyridine) (PVPy) or poly(butyl acrylate-*co*-4-vinyl pyridine) (BVPy) and mono-carboxy terminated polystyrene (MCPS). The hydrogen-bonding interaction was evidenced by ^{13}C NMR and FT-IR. In the blend solution, the grafting of MCPS onto PVPy or BVPy backbones led to graft-like complexes showing much larger average hydrodynamic radius (R_h) than is shown by either component alone, the conformation of PVPy backbone undergo chain extension due to the steric repulsion of grafted MCPS chains. Moreover, both viscometry and LLS showed a strong effect of molar mass of MCPS on grafting, e.g. the number of branches on each PVPy backbone decreased from 330 to 3 as the molar mass increased from 1.8k to 23.4k. Fluorescence measurements in the blend solutions supported these conclusions. The DSC results of PVPy/MCPS blends in bulk showed two-phase structures as the hydrogen bonding interaction existing between carboxyl end and PVPy is not enough to cause complete mixing. Besides, the thermal history greatly influenced the phase behavior of the blends as the hydrogen bonding is sensitive to temperature. For the blends containing MCPS and BVPy-34 with lower VPy content and much lower T_g , miscibility over the whole composition range was obtained. © 2000 Elsevier Science Ltd. All rights reserved.

Keywords: Graft-like complexes; Hydrogen bonding; End-functionalized oligomers

1. Introduction

It has been our interest to study interpolymer complexes via hydrogen bonding as an extension of our long-term studies on miscibility enhancement by introducing hydrogen bonding into polymer blends [1]. Our previous work shows that for an otherwise immiscible blend pair, not only miscibility but also complexation between the components can be realized as the interpolymer hydrogen bonding is intensified [1–12]. The proton-donating polymers employed include styrene-based carboxyl containing polymers, i.e. carboxylated polystyrene (CPS) [3] and a series of hydroxyl containing polymers such as poly[styrene-*co*-(*p*-vinylphenol)] (STVPh) [4–7], poly[styrene-*co*-(*p*-1-hydroxyethyl)styrene] (PS(2-OH)) [8] and poly{styrene-*co*-[*p*-2,2,2-trifluoromethyl)ethyl]- α -methylstyrene} (PS(OH)) [9–12]. The proton-accepting polymers employed include pyridyl or carbonyl containing polymers. For instance, for the immiscible blends of PS/poly(butyl methacrylate-*co*-4-

vinyl pyridine)-50 (BVPy-50), only 1.8 mol% of –COOH randomly introduced into PS chain rendered the miscibility, and more importantly, complexation between CPS and BVPy-50 was observed as the carboxyl content in CPS further increased to 7 mol%, i.e. one carboxyl among about 14 units of styrene [3]. This kind of complexation both in solution and bulk was clearly explored and confirmed by viscometry, laser light scattering (LLS) and nonradiative energy transfer (NRET) fluorospectroscopy.

Generally, complexation in solutions between homopolymers or random copolymers with the interaction groups randomly distributed on the polymer chain is accompanied by segment-pairing and leads to precipitates with ill-defined structure. This, of course, causes difficulties when we examine the complexation process and explore the structure of complexes. Moreover, since specific interaction groups are introduced into the polymer chain through copolymerization or chemical modification, the distribution of the groups is difficult to be controlled, this has given rise to further obstacles in the study of the structure of interpolymer complexes. Thus, our current research on interpolymer complexation is aimed at obtaining soluble complexes with some relatively well-defined structures.

* Corresponding author. Tel.: + 86-21-6564-3919; fax: + 86-21-6564-0293.

E-mail address: mjiang@fudan.ac.cn (M. Jiang).

It was reported that end-functionalized oligomers can be complexed to ionomers by ionic bonding to produce graft-like complexes. Weiss et al. [13] studied the lightly sulfonated polystyrene (PS-SSA)/tertiary amine-terminated isoprene oligomers. Bauzuin et al. studied the blends of PS-SSA and tertiary amine-terminated polystyrene [14] or poly(*tert*-butyl acrylate) oligomers where the amine groups can interact with sulfonate groups through proton-transfer [15]. In the former, the backbone and grafts are basically the same in chemical structure, while in the latter, they are different. They are called as homografts and heterografts, respectively. It was found that in the homografts, the monofunctional oligomers plasticize the materials to an extent depending on the length and stiffness of the side chains, and the longer bifunctional oligomers present a biphasic material despite the ionic contacts between, and segmental identity of the two components. In the heterografts, the dynamic mechanical analysis shows only marginal phase separation.

To our knowledge, there were no experimental reports about the graft-like complexes, in which the oligomer is attached to the homopolymer backbone through reversible specific interactions such as hydrogen bonding. As the first paper of our research on such hydrogen-bonded graft-like complexes, our recent communication [16] presents results for blend solutions comprising of polystyrene oligomers with end groups of mono-carboxy (MCPS) or di-carboxy (DCPS) and poly(4-vinylpyridine)PVPy. Both viscometry and dynamic light scattering clearly indicated the formation of the stable, soluble complexes with PVPy backbone and MCPS or DCPS grafts. The two carboxyl groups in DCPS provide much stronger ability for complexation than does the single carboxyl end in MCPS. Based on this finding, we have extended our work to the blends containing oligomers with different end groups such as $-\text{C}(\text{CF}_3)_2\text{OH}$, $-\text{CH}_2\text{OH}$, $-\text{COOH}$ and $-\text{N}(\text{CH}_3)_2$. Our particular interest at the moment concerns the effects of the molar mass of the mono-carboxy terminated polystyrene (MCPS). As the carboxyl group is located only at one chain end of polystyrene, the variation of molar mass simultaneously changes the density of carboxyl groups on the polymer chain. We altered the molar mass of MCPS, and consequently, the carboxyl content on the PS chain, and modulated the pyridyl content by copolymerizing it with inert monomers such as butyl acrylate. The use of butyl acrylate as a comonomer is due to its low T_g (-54°C) and its having very weak interaction with carboxyl [3]. Besides the solution properties investigated by viscometry, LLS and NRET fluorospectroscopy, the studies have focused on the morphology and properties of such complexes in bulk as well.

2. Experimental

2.1. Materials

4-Vinyl pyridine (VPy), styrene, butyl acrylate were

vacuum distilled in the presence of calcium hydride just before use. Vinylcarbazole, purchased from Aldrich, was used as received without further purification. The energy-acceptor monomer, 9-anthrylmethyl methacrylate was synthesized from 9-hydroxymethyl anthracene and methacryloyl chloride in the presence of triethyl amine and anhydrous pyridine followed by column chromatography purification.

2.2. Preparation of MCPS [16,17]

Anionic polymerization of styrene was carried out at -20°C in benzene/THF (3/1) using *n*-BuLi in cyclohexane (about 1.0 M) as the initiator. The living polystyryl was terminated by CO_2 free of oxygen and protonic impurities. The crude product was then purified by passing through silicon gel columns. FT-IR of MCPS shows a strong carbonyl stretching peak at 1706 cm^{-1} . ^{13}C NMR shows a signal of carbonyl at 179 ppm. The functionality of MCPS was calculated from the results of SEC and acid–base titration using $\text{NaOCH}_3/\text{toluene}$.

2.3. Preparation of poly(4-vinyl pyridine) (PVPy) and chromophore-labelled PVPy

Poly(4-vinyl pyridine) (PVPy) was prepared by anionic polymerization in THF using naphthalene sodium as the initiator. The product was purified in methanol/ethyl ether cycle three times. The molar mass of PVPy was calculated from intrinsic viscosity ($[\eta]$ (in dl/g)) data in absolute ethanol using $[\eta] = 2.5 \times 10^{-2} \times M_\eta^{0.68}$. Anthracene-labeled and carbazole-labeled PVPy were produced through radical copolymerization of 4-vinyl pyridine and 9-anthrylmethyl methacrylate (AMMA) or vinyl carbazole. The chromophore contents in PVPy-a and PVPy-c (a and c denote PVPy labeled with AMMA and vinyl carbazole units, respectively) were determined by UV spectroscopy and both were found to be 0.24 wt%.

2.4. Preparation of poly(butyl acrylate-co-4-vinyl pyridine) (BVPy)

BVPy was prepared by bulk copolymerization of butyl acrylate and 4-vinyl pyridine using AIBN as the initiator at 60°C . The total conversion of the monomers was kept at less than 15% and the molar contents of VPy in BVPy were obtained from nitrogen measurements. The molar mass of BVPy was determined by SEC using polystyrene as calibration standard.

2.5. Characterization

Infrared spectra were obtained with a Nicolet Magna 550 FT-IR spectrometer. Thirty-two scans were taken, corresponding to a resolution of 2 cm^{-1} . The samples were thin films cast from CHCl_3 onto NaCl plates and vacuum dried.

NMR measurements were performed on a Bruker

Table 1
Characteristics of the samples used in this study

Samples ^a	<i>n</i> ^b	<i>M_n</i> (10 ³ g/mol)	<i>M_w/M_n</i>	<i>f</i> ^c	<i>T_g</i> (°C)
MCPS-1.8	17	1.8	1.28	0.95	86
MCPS-2.2	21	2.2	1.19	0.88	88
MCPS-3.9	38	3.9	1.16	0.91	93
MCPS-5.5	53	5.5	1.06	0.98	97
MCPS-23.4	225	23.4	1.06	0.90	102
PS-2.3	22	2.3	1.14	–	63
PVPy	1330	140 ^d	–	–	151
PVPy-a ^e	1190	125 ^d	–	–	–
PVPy-c ^e	1140	120 ^d	–	–	–
BVPy-34 ^f	/	120	1.45	–	9
BVPy-50 ^f	/	110	–	–	39

^a The numerals in sample code MCPS-*x* denote the molar mass of MCPS.

^b *n* is the average number of units per chain.

^c *f* denotes functionality.

^d Calculated from intrinsic viscosity data.

^e *a* and *c* denote PVPy labelled with AMMA and vinyl carbazole units, respectively.

^f The numerals after the hyphen in BVPy-*x* denote the mole content of VPy in the copolymers.

MSI-300. The ¹³C NMR spectra were acquired from 4% solution in CDCl₃.

The viscosities of the polymer blend solutions in CHCl₃ were measured with an Ubbelohde viscometer at 25 ± 0.1°C. The original concentration of the individual polymer was 4.0 to 10 × 10⁻³ g/ml. Measurements of the reduced viscosities of PVPy/MCPS blends as a function of the composition were conducted via mixing solutions of PVPy and MCPS as desired.

2.6. Laser light scattering

A modified commercial LLS spectrometer (ALV/SP-125) equipped with a multi-*λ* digital time correlator (ALV-5000e) and a solid-state laser (ADLAS DPY425 II, output power ≅ 50 mW, at λ₀ = 532 nm) was used. The incident beam was vertically polarized with respect to the scattering plane. All measurements were measured at 25.0 ± 0.1°C.

In dynamic LLS, the intensity–intensity time correlation function $G^{(2)}(q,t)$ is measured in the self-beating mode, and $G^{(2)}(q,t)$ has the following relationship to the normalized first-order electric field time correlation function $|g^{(1)}(q,t)|$.

$$G^{(2)}(q,t) = \langle I(0,q)I(t,q) \rangle = A(1 + \beta |g^{(1)}(q,t)|^2) \quad (1)$$

where *A* is a measured baseline, β an instrument parameter depending on the coherence of detection and *t* the delay time. For a polydisperse sample, $|g^{(1)}(q,t)|$ is related to the linewidth distribution $G(\Gamma)$ as

$$|g^{(1)}(t,q)| = \langle E(0,q)E^*(t,q) \rangle = \int_0^\infty G(\Gamma) e^{-\Gamma t} d\Gamma \quad (2)$$

$G(\Gamma)$ can be calculated from the Laplace inversion of $G^{(2)}(t,q)$ on the basis of Eqs. (1) and (2). In this study, the constrained regularization CONTIN program developed by

Provencher was used. For a diffusive relaxation, Γ is a function of both *C* and *q*, namely $\Gamma/q^2 = Df(C,q)$, where *D* is the translational diffusion coefficient at $C \rightarrow 0$ and $q \rightarrow 0$. Therefore, for a dilute solution at a small scattering angle, $\Gamma/q^2 \approx D$. Further, *D* can be converted to the hydrodynamic radius (*R_h*) using the Stokes–Einstein equation: $R_h = k_B T / 6\pi\eta D$, where η is the solvent viscosity, *k_B* the Boltzmann constant, and *T* the absolute temperature.

2.7. Fluorescence measurements

Emission spectra of the polymer solutions were recorded on a FZ-1 fluorescence spectrometer at room temperature (ca 25°C). The component polymer solutions were prepared with oxygen-free solvents. The total concentration of PVPy-a, PVPy-c in CHCl₃ was kept at 1.0 × 10⁻³ g/ml. Blend solutions were prepared by mixing the corresponding polymer solutions at a weight ratio of PVPy-a/PVPy-c/MCPS 1/1/20 in a quartz cell with stirring, and purged with nitrogen for at least 1 min before each recording. The wavelength of the excitation light was set at 294 nm, and the direction of the excitation light was perpendicular to that of the emission detected. The energy transfer was characterized by I_c/I_a , the ratio of the emission intensity at 365 nm (*I_c*) to that at 416 nm (*I_a*), which were mainly due to the contributions from the energy-donor carbazole and the energy-acceptor anthracene, respectively.

2.8. Differential scanning calorimetry

Polymer blends for differential scanning calorimetric (DSC) measurements were prepared by solvent casting: 3% solutions of the component polymers in chloroform were mixed, stirred for 8 h at room temperature before the solvent was allowed to evaporate out slowly at ambient temperature for 3 days. Final drying of films formed was done under vacuum at 70°C.

DSC measurements were conducted with a differential scanning calorimeter (DSC-50, Shimadzu). The heating rate was 10°C/min and samples of about 10 mg in a sealed alumina cell were measured under a nitrogen gas atmosphere. Two thermal programs were used, i.e. in the quenching program, the sample was heated to and then kept at 180°C for 15 min followed by quenching in liquid nitrogen for several minutes and in the annealing program, the sample was heated to and kept at 180°C for 15 min followed by cooling to 25°C at a rate of 1°C/min.

2.9. Transmission electron microscopy

Transmission electron microscopic (TEM) observations were performed on a Philips EM400ST transmission electron microscopy at an accelerating voltage of 80 kV. Thin films were cast from CHCl₃ onto 200-mesh carbon-coated grids. The PVPy phase was preferentially stained in iodine vapor.

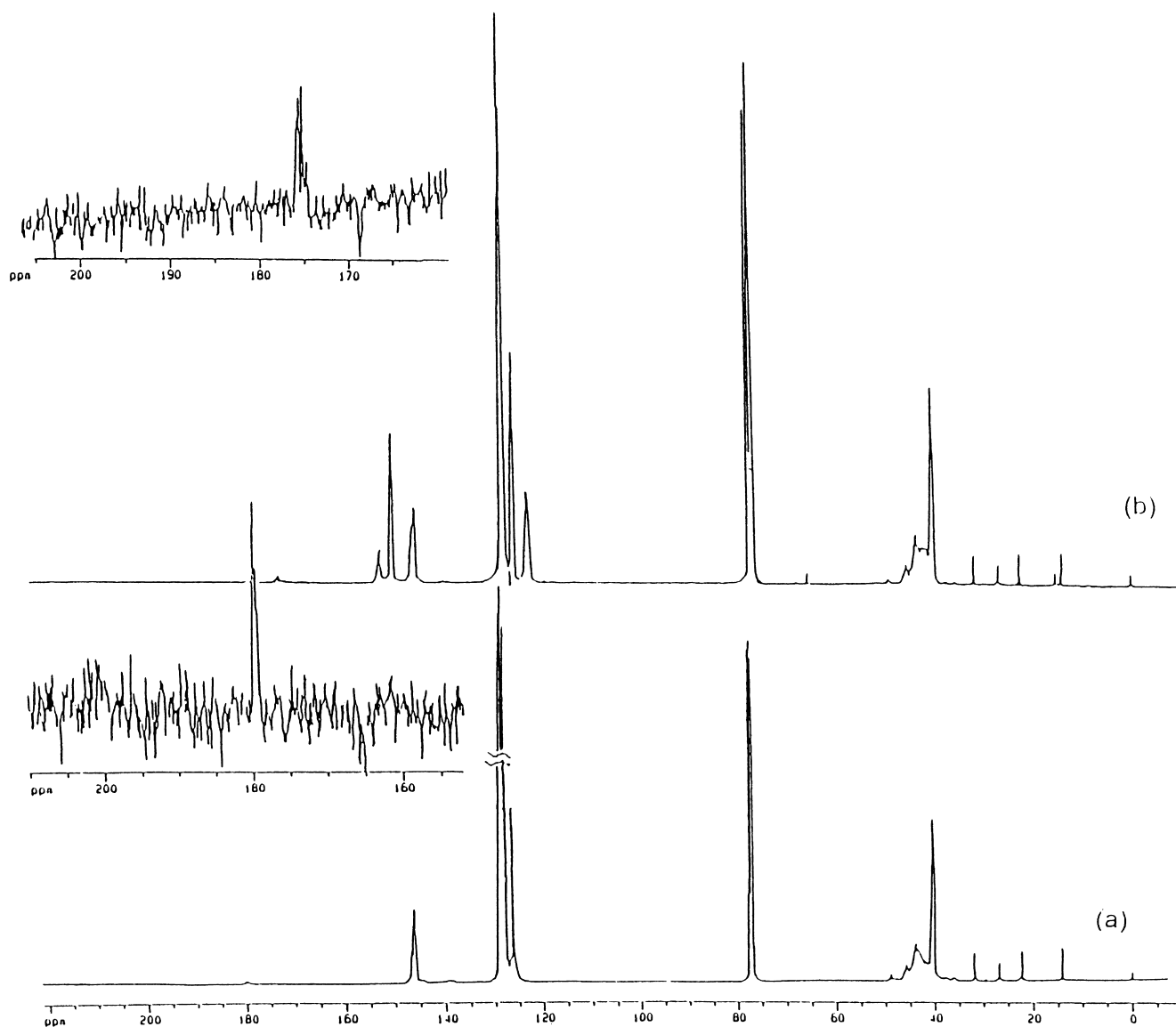


Fig. 1. The ^{13}C NMR spectrum of MCPS-1.8 and the blend solution of PVPy/MCPS-1.8 (1:2 wt/wt).

3. Results and discussion

3.1. Spectral characterization of the hydrogen bonding interaction

The characteristics of the samples used in this study are listed in Table 1. A polystyrene homopolymer with a molar mass of 2300 was used as a reference.

Fig. 1 shows the ^{13}C NMR spectra of MCPS-1.8 and its blends with PVPy (1/1 wt/wt). Pure MCPS-1.8 shows a signal of carboxyl carbon at 179 ppm. In the blend solution, the signal of carboxyl carbon shifts to high field at 176 ppm. This reflects the fact that the self-association of carboxyl in MCPS chains is disrupted by the formation of intermolecular hydrogen bonding between carboxy hydroxyl and pyridyl leading to the carboxyl carbonyl being free.

The IR spectrum also qualitatively reflects the hydrogen bonding interaction between pyridyl and carboxyl in the solid state, as the carboxy carbonyl in MCPS is freed from the carboxyl self-association when pyridyl interacts with the carboxy hydroxyl. In the present case, since the carboxyl content is very low, namely, one carboxyl per chain, the carboxyl may have relatively weak self-association. Fig. 2 shows the IR spectrum of MCPS, PVPy and its blends of PVPy/MCPS (1:2 wt/wt). The pure MCPS shows a sharp carbonyl peak at 1706 cm^{-1} , while its blends with PVPy show a broad carbonyl peak at 1713 cm^{-1} . The shift and widening of the carbonyl peak is obviously as a result of the interaction between the pyridyl and the carboxyl. It is understandable that the characteristic peaks of PVPy such as $1597, 996\text{ cm}^{-1}$ in the blends almost remain the same, since the carboxyl/pyridyl mole ratio in PVPy/MCPS-1.8 (1:2 wt/wt) blends is very low and if PVPy/MCPS blends

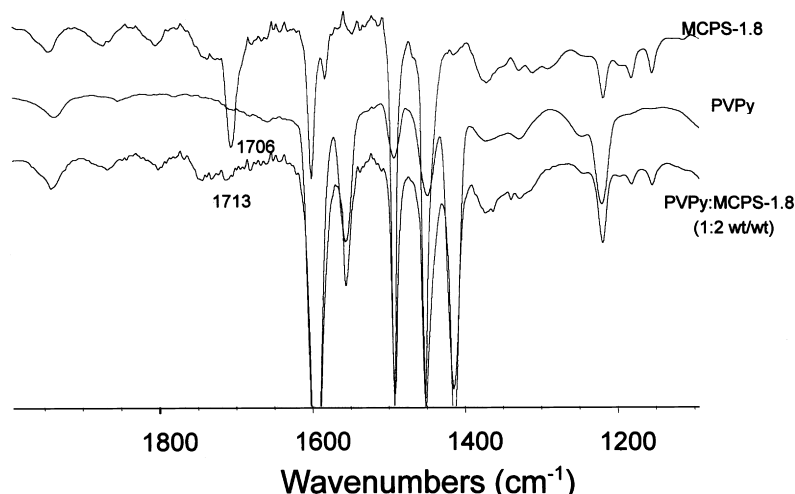


Fig. 2. The IR spectra of PVPy, MCPS-1.8, and their blends PVPy/MCPS-1.8 (1:2 wt/wt).

are phase separated in bulk, the number of pyridyl hydrogen bonded will be even lower.

3.2. Complexation in solution

3.2.1. Viscosity behavior

The variation of reduced viscosity of polymer blends with the blend composition has been empirically used as a criterion of complex formation [1]. This is based on the following fact: for blend solutions with a concentration below its overlap concentration C^* , if there are no specific interactions between the polymer chains, the chains are expected to remain separated and behave independently and so the viscosity of the solutions follows the additive law. Otherwise, the viscosity may show a deviation, positive or negative, from the additivity. Fig. 3 shows the reduced viscosity of the blend solutions of PVPy and MCPS with different molar masses of 1.0k, 1.8k, 3.9k and 5.5k in CHCl_3 , which is almost inert to hydrogen bonding, as a function of the blend composition. The C^* estimated by $C^* = 1/[\eta]$ for PVPy in CHCl_3 should be higher than 0.019 g/ml and 0.1 g/ml for MCPS, respectively. So in the measurements, a much lower concentration of 0.01 g/ml was used. The viscosity behavior of the control, i.e. PVPy/PS-2.3 blend solutions was found to obey the additivity law. In contrast, all the blend solutions of PVPy/MCPS-1.8, PVPy/MCPS-3.9 and PVPy/MCPS-5.5 clearly showed a positive deviation from the additivity law. This deviation can obviously be attributed to the intermolecular complexation. Since the MCPS oligomers have proton-donor groups at one chain end only, it was expected that the active end groups in the solutions will attach to PVPy chain to form graft-like complexes. Moreover, different from the case of “conventional complexation” from different polymers with interaction sites randomly distributed along the polymer chains, which is always accompanied by precipitation, all of the blend solutions of PVPy/MCPS remain clear at any composition. It means that this is a new type of soluble “graft-like”

complexes in which only hydrogen bonds rather than chemical bonds exist between the backbone and grafts. The complexation of the polymer with end-functionalized oligomers leads to an increase of hydrodynamic volume relative to the pure components, as shown by the increase in viscosity. This is different from all the conventional complexation process we observed previously which is always accompanied by chain collapse, leading to a decrease of viscosity [1].

Fig. 3 compares the reduced viscosity of blend solution of PVPy and MCPS with different molar mass. Generally, a decrease of the MCPS molar mass can lead to a larger increase in the reduced viscosity. This effect appears more evident for solutions in which MCPS is the predominant component. In fact, a decrease of the molar mass of MCPS implies an increase of the relative carboxyl content in the polystyrene chain, and a lessened steric hindrance in its grafting to the backbone. Obviously, the two factors will make more MCPS attach to the backbone.

We have also studied the effect of pyridyl content on

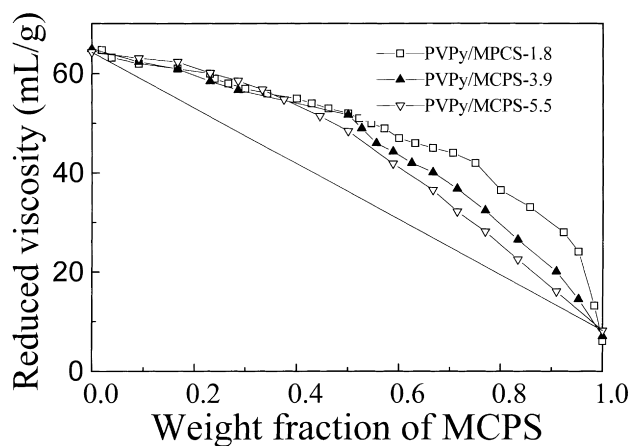


Fig. 3. Reduced viscosity of the blends of PVPy and MCPS with different molar mass in CHCl_3 versus weight fraction of MCPS. The total concentration is 10×10^{-3} g/ml.

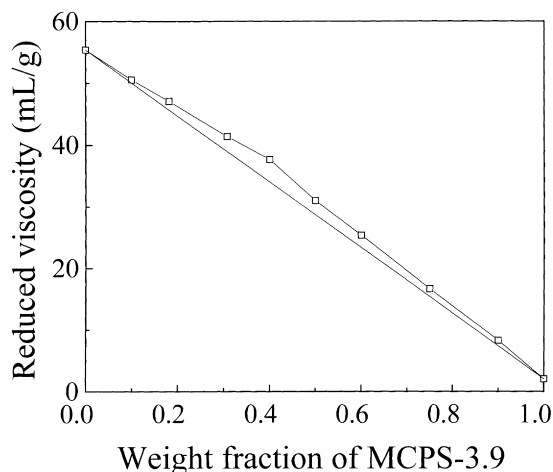


Fig. 4. Reduced viscosity of the blend of BVPy-50 and MCPS-3.9k in CHCl_3 versus the weight fraction of MCPS-3.9. The total concentration is 4×10^{-3} g/ml.

complexation. Fig. 4 shows the reduced viscosity of the blend solutions of BVPy-50 and MCPS-3.9 as a function of the weight fraction of MCPS-3.9. The blend solution showed a much smaller positive deviation from the additivity law than did PVPy/MCPS-3.9. It was reported that carboxyl has very weak interactions with ester carbonyl [3], so copolymerizing vinyl pyridine with an inert comonomer such as butyl acrylate weakens the complexation between the backbone and MCPS.

The reduced viscosities of the solutions of MCPS, PVPy and their blends as functions of the concentration were measured. It is interesting to see that the blend solution which actually contains both the “graft copolymers” and the “free” chains show linear relationship between η_{sp}/C and C . It means that the graft copolymers are actually stable in solution. The measured intrinsic viscosities $[\eta]$ of the blends, the corresponding calculated values based on additivity and their difference are listed in Table 2. At both compositions of PVPy/MCPS 1/1 and 1/9, the data show that increasing the molar mass of MCPS decreases the effect of viscosity increment caused by the hydrogen-bonding complexation.

3.3. Laser light scattering studies

LLS has been proved to be powerful in making a direct view of different kinds of macromolecular assembly in solutions [1,18]. Fig. 5 displays the apparent hydrodynamic

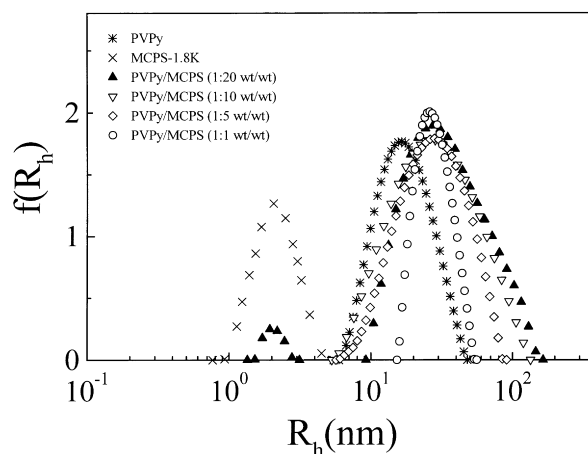


Fig. 5. Hydrodynamic radius distribution of PVPy, MCPS-1.8, and their blend solutions with different composition.

radius distributions $f(R_h)$ of pure MCPS-1.8, PVPy and their blends with different compositions in CHCl_3 at a total concentration of 1×10^{-3} g/ml. Pure MCPS and PVPy show hydrodynamic radius (R_h) distribution peaks located at around 2 and 17 nm, respectively. Although MCPS has a narrow polydispersity index determined by SEC in THF, it shows a relatively broad distribution of R_h in CHCl_3 ranging from around 1 to 4 nm, which probably implies the coexistence of the single MCPS chain, its dimers and multimers formed by self-association of carboxyl in chloroform which is almost inert to hydrogen-bonding.

For the blend solutions, the most remarkable feature observed is the appearance of a relatively broad distribution of R_h with peaks at $R_h \sim 27$ nm, much higher than either MCPS or PVPy alone. No doubt, the high R_h peak is associated with the graft-like copolymers. When the weight ratio of PVPy/MCPS goes from 1/1 to 1/20, the larger R_h side of the distribution curve shifts to higher R_h values indicating that more MCPS have been grafted onto PVPy backbones. Since the average radius of the graft complex is almost 10 times higher than that of MCPS and light scattering is much more sensitive to large than to small particles, the absence of the peak around 2 nm for the case of PVPy/MCPS 1/1, 1/5 and 1/10 does not necessarily exclude the existence of free MCPS. However, when the weight ratio of MCPS to PVPy reaches 20:1, the peak associated with free MCPS becomes detectable. It means that the PVPy chains are “saturated” with the MCPS grafts.

Table 2
The intrinsic viscosities (ml/g) for PVPy/MCPS blends with different weight composition

Blends	1:1			1:9		
	Calculated	Measured	$\Delta\eta_{sp}/C$	Calculated	Measured	$\Delta\eta_{sp}/C$
PVPy/MCPS-1.8	29.8	35.2	5.4	11.7	16.9	5.2
PVPy/MCPS-3.9K	30.7	34.5	3.8	12.1	15.7	3.6
PVPy/MCPS-5.5K	31.2	34.0	2.8	12.6	14.8	2.2

Table 3

$\langle R_h \rangle$ of the complexes and the estimated grafts number per PVPy chain of the blend solutions of PVPy/MCPS (1/10 wt/wt) with different molar mass

Blend solutions	MCPS-1.8	MCPS-3.9	MCPS-5.5	MCPS-23.4
$\langle R_h \rangle$ (nm)	27	25	24	19
Grafts number per PVPy chain	233	78	47	3

The following fact is worth noting. As mentioned above, complexation between MCPS and PVPy causes a substantial increase in reduced viscosity relative to the additivity value. However, even in the case with the highest increment in reduced viscosity (PVPy/MCPS-1.8 1/2), the viscosity of the blend solution is still apparently lower than that of PVPy. In contrast, either the R_h peak value or the average value $\langle R_h \rangle$ of the blend solutions, over the whole composition range, is much higher than that of PVPy. Considering that the viscosity is an overall reflection of both the large graft copolymers and small free-MCPS, while in the light scattering the large molecules always make predominant contribution to the scattering intensity, this superficial difference turns to be understandable.

Attaching MCPS to PVPy backbone is no doubt the main factor responsible for the R_h increase. The conformational change, i.e. chain extension of the PVPy backbone due to the steric repulsion caused by the grafted MCPS chains [19,20] may make a little contribution as well.

Over the whole composition range in our LLS experiments, i.e. PVPy/MCPS-1.8 from 1:1 to 1:20, the ratio of the chain number of MCPS to pyridyl units in PVPy varies from 78:1 to 1555:1. Thus it is reasonable to assume that in forming a complex, PVPy chains may play the role of “nuclei” and each complex molecule contains one PVPy chain. From the R_h values of PVPy and complex molecules, we are able to make a rough estimation of the composition of the complex molecules. For example, for PVPy/MCPS-1.8 1/10 blends, based on the $\langle R_h \rangle$ values, the hydrodynamic volume ratio of the complex molecule to PVPy is found to be 4. Assuming that the chain density is about the same in

pure PVPy and in the complex, the molar mass of the complex can be estimated to be 5.6×10^5 and consequently, on an average, there are about 233 MCPS chains attached to one PVPy chain. The same estimation was made for all the blend solutions containing MCPS of different molecular weights and the results are summarized in Table 3.

A remarkable decrease in the number of MCPS grafts with increasing molecular weight is observed, e.g. the graft number per PVPy chain decreased from 233 to 3 when the molar mass of MCPS increased from 1800 to 22,300. We have no intention to emphasize the changes quantitatively, however, it does indicate the importance of the effect of molecular weight and the consequent steric hindrance of the branches in forming hydrogen-bonding graft complex.

We also found by dynamic light scattering that in the blend solutions of MCPS and BVPy-50 (50% VPy molar content), graft complex forms as well but with $\langle R_h \rangle$ increment much smaller than the corresponding PVPy/MCPS blends. This is expected and is in agreement with the viscosity data.

In one of our previous papers [3], we reported the complexation between BVPy and partially carboxylated polystyrene (CPS) in which functional groups $-\text{COOH}$ are randomly distributed rather than at chain end only. Regarding the complex formation, the random copolymer requires much higher carboxyl content than MCPS does. This means that the functional group at the end possesses a much stronger ability to attach into a backbone than those at the other positions. It is understandable since the end group is usually more mobile and causes less steric hindrance than those in the middle of the chains.

3.4. Nonradiative energy transfer fluorescence studies

The NRET fluorescence spectroscopy used here is based on the fact that the efficiency of the energy transfer (denoted as I_c/I_a) between a fluorescence energy donor and acceptor depends strongly on their proximity over a scale of ~ 2 – 4 nm. Therefore, I_c/I_a is expected to reflect the distance and degree of interpenetrating of a pair of polymers provided the components are labeled with energy donor and energy acceptor, respectively. In this study, PVPy labeled with the energy donor (PVPy-a) and energy acceptor groups (PVPy-c) were used.

Fig. 6 shows the I_c/I_a dependence of PVPy-a/PVPy-c/MCPS-1.8 blend solutions on the concentration of MCPS where the total concentration of PVPy-a and PVPy-c was kept constant at 1×10^{-3} g/ml and the ratio of PVPy-a/PVPy-c

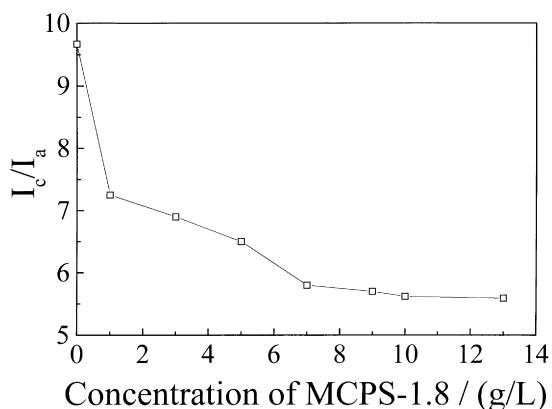


Fig. 6. Variation of I_c/I_a of blend solutions of PVPy-a/PVPy-c/MCPS-1.8k in chloroform with the concentration of MCPS-1.8. The total concentration of PVPy-a and PVPy-c was 1×10^{-3} g/ml, and the weight ratio of PVPy-a and PVPy-c was 1/1.

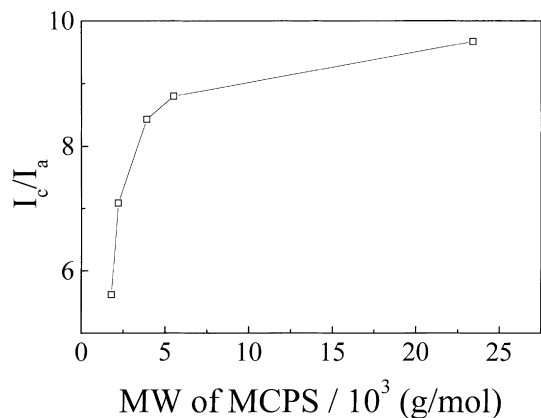


Fig. 7. I_c/I_a variation of blend solutions of PVPy-a/PVPy-c/MCPS (weight ratio 1/1/20) in chloroform with the molar mass of MCPS. The total concentration of PVPy-a and PVPy-c was 1×10^{-3} g/ml, and the weight ratio of PVPy-a and PVPy-c was 1/1.

was 1/1 to keep the $[c]/[a]$ constant. I_c/I_a decreases considerably on the increase of concentration of MCPS-1.8 indicating that energy donor and acceptor on different PVPy chains have larger possibility to come close to each other in the blend solutions. As mentioned above, in the blend solutions, PVPy chains existing in the “graft copolymer” aggregates have much larger R_h than that of the pure PVPy chain. For example, in the solutions of PVPy/MCPS-1.8 (1/10 wt/wt), the hydrodynamic volume ratio of the “graft copolymer” to the pure PVPy is about 4, as we discussed also, this is partially because the grafting of MCPS onto PVPy chains makes the PVPy chains adopt more extended conformations. Obviously, both the volume increase of hydrogen bonded “graft-like” complexes and the chain extension of the PVPy backbone favor the dynamic contact of fluorescence donor and acceptor groups on different PVPy chains, leading to an increase of the NRET efficiency.

It can also be seen from Fig. 6 that I_c/I_a almost no longer

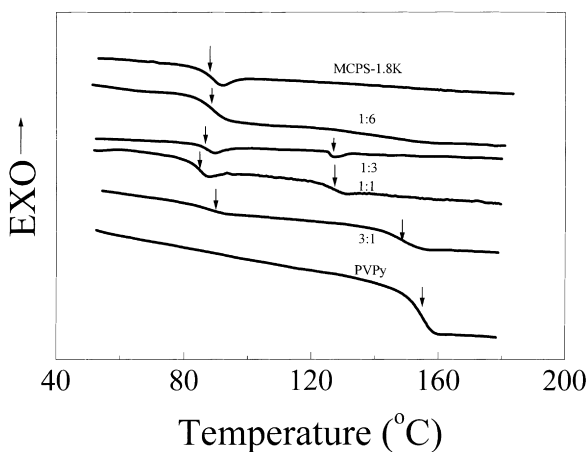


Fig. 8. DSC thermograms of PVPy/MCPS-1.8 blends with different blend compositions (PVPy/MCPS-1.8, wt/wt). The samples were heated to, and kept at 180°C for 15 min followed by cooling to 25°C at a rate of 1°C/min.

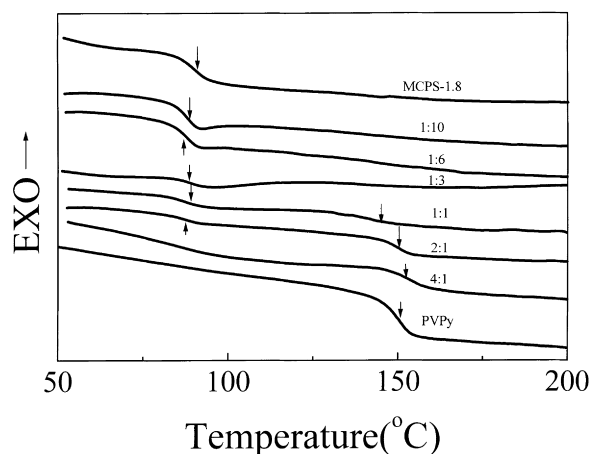


Fig. 9. The DSC thermograms of PVPy/MCPS-1.8 with different blend compositions (PVPy/MCPS-1.8, wt/wt). The samples were heated to and then kept at 180°C for 15 min followed by quenching in liquid nitrogen.

decreases as the weight ratio of MCPS-1.8/PVPy reaches the range around 7/1 to 10/1. This implies that over this weight ratio range, the PVPy backbone was saturated with MCPS-1.8 chains. In other words, the steric repulsion between the grafted MCPS chains made further grafting impossible. This was generally in agreement with the conclusions made by the LLS measurements as mentioned above.

Fig. 7 shows the dependence of molar mass of MCPS on I_c/I_a of the PVPy/MCPS blend solutions in CHCl_3 composed of PVPy-a/PVPy-c/MCPS at a weight ratio of 1/1/20. Note that the variation of molar mass of MCPS chain changes the carboxyl content simultaneously. A general feature of Fig. 7 is that the higher the molar mass of MCPS is, the larger is the I_c/I_a value. This indicates that increasing the molar mass of MCPS lessens the increase of the hydrodynamic volume and the chain extension of PVPy. In fact, as for the blend solutions containing MCPS with the highest molar mass of 2.34×10^4 , the I_c/I_a value turns to be the same as the solutions only containing PVPy-a and PVPy-c. This means that almost no complexation occurs between PVPy and MCPS-23.4 as the carboxyl content in the MCPS-23.4 is very low and the shielding effect of the long PS chains on the accessibility of the end carboxyl to pyridyl units is very effective.

3.5. Phase behavior studied by thermal analysis

Now we move to the bulk properties of the complexes. The T_g data of the individual component polymers measured by DSC are listed in Table 1. We can see that the introduction of carboxyl group into polystyrene chain end prominently increased the T_g of MCPS compared to the parent polystyrene. The T_g increase depending on the molecular weight is about 20–30°C, which can be obviously attributed to the self-association of carboxyl end groups retarding the chain mobility.

The DSC thermograms of the annealed and quenched

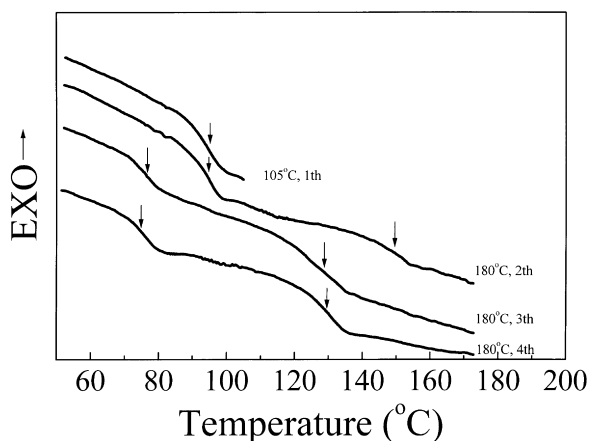


Fig. 10. The DSC thermograms of PVPy/MCPS-3.9 (1:1 wt/wt) in a successive thermal treatment. 1st–4th denotes the heating sequence, the sample was cooled to room temperature after each run.

PVPy/MCPS-1.8 blend samples are shown in Figs. 8 and 9, respectively. In all cases, the blends exhibit two T_g s, indicating phase separation between the PVPy-rich phase and MCPS-rich phase. Since only the end of the MCPS chain has the favorable interaction with PVPy chain, phase separation is expected. In Fig. 8, depending on the blend composition, T_g of the PVPy-rich phase decreases by about 5–20°C and reaches its lowest as the blend ratio is between 1/1 and 1/3 (PVPy/MCPS-1.8). In this composition range, PVPy/MCPS-1.8 blend solution also gave the largest positive deviation in the viscosity measurement. Thus, the introduction of carboxyl onto the polystyrene chain end clearly improves the phase mixing between PS and PVPy. For reference, it was observed that, for the PVPy/PS-2.3 blends (data not shown), the two T_g s are closely correspond to those of pure PVPy and PS, respectively, indicating almost no phase mixing.

It is interesting to note that although T_g of PVPy is about

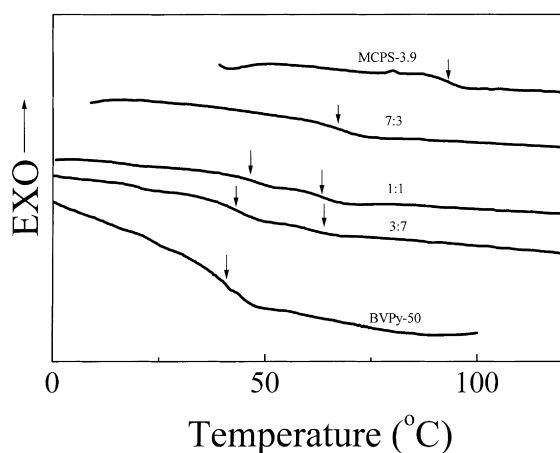


Fig. 11. DSC thermograms of BVPy-50/MCPS-3.9 with different blend compositions (MCPS-3.9/BVPy-50, wt/wt). The samples were heated to and kept at 120°C for 15 min followed by cooling to low temperature at a rate of 1°C/min.

60°C higher than that of MCPS-1.8, in the blends, depending on the composition, the MCPS-rich phase either shows a decrease or an increase of T_g compared to that of pure MCPS. For example, as shown in Fig. 8, T_g of MCPS-rich phase is 5°C lower and 3°C higher than that of pure MCPS for blends of PVPy/MCPS-1.8 wt/wt 1:1 and 3:1, respectively. In our opinion, the change in T_g of MCPS-rich phase observed for the blends is a result of competition between two factors: the interaction between pyridyl and hydroxyl disrupting the self-association of carboxyl causing a decrease in its T_g and meanwhile, incorporating the high- T_g PVPy chains into MCPS phase resulting in an increase of T_g .

Fig. 9 shows the DSC thermograms of the blends of PVPy/MCPS-1.8 with different compositions quenched from 180°C. Compared to that in Fig. 8 we can see that there still exist two T_g s, but the T_g shifts are much smaller. This indicates that the heat treatment to 180°C may have caused disruption of hydrogen bonding leading to complete phase separation. The effect of thermal history on the phase behavior can be seen in more detail from the DSC thermograms of PVPy/MCPS-3.9 (1/1 wt/wt) blends measured in a sequence of heat treatment as shown in Fig. 10. On the first heating to 105°C of the sample without prethermal treatment, the T_g obviously corresponding to the MCPS-rich phase was observed at 95°C. After cooling the sample we heated it to 180°C, two T_g s located at 149°C and 94°C, very close to the pure PVPy and MCPS-3.9 were detected, which indicates that phase separation in the as-prepared blend samples is nearly complete. After slow cooling of the samples at 1°C/min to 25°C, the sample was again heated to 180°C, and it showed a remarkable change, i.e. the two T_g s shift down to 127°C and 76°C, respectively, indicating a certain amount of phase mixing. Further cooling and heating shows nearly the same T_g value. This reflects the fact that, although the hydrogen bonding is partially disrupted when the temperature is as high as 180°C, it can be re-established in the process of slow cooling leading to a rearrangement of the polymer chains and some extent of phase mixing.

In the DSC measurements of PVPy/MCPS blends, since the T_g of PVPy is 151°C, the hydrogen bonding between the two components is expected to be unavoidably affected as the temperature is raised above the T_g of PVPy. This problem can be avoided by using BVPy copolymers instead of PVPy, with much lower T_g compared to pure PVPy. In this way, we can examine the effect of the end carboxyl at the PS chain on its miscibility enhancement with VPy-containing copolymers in a relatively low temperature range (<100°C). Fig. 11 shows the DSC thermograms of BVPy-50/MCPS-3.9 blends. Pure BVPy and MCPS-3.9 show T_g s at 39 and 94°C, respectively. It is remarkable to see that BVPy-50/MCPS-3.9 (3/7) show only one T_g at 68°C, which is intermediate between the two pure components indicating the miscibility over phase size of tens of nanometers. The 1/1 and 7/3 blends show two T_g s associated with the MCPS-rich and BVPy-rich phases, respectively,

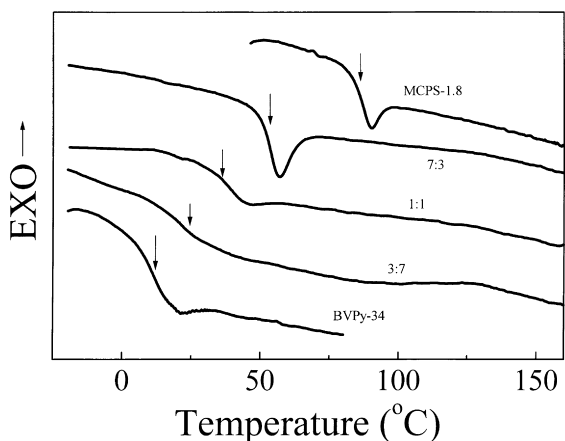


Fig. 12. DSC thermograms of BVPy-34/MCPS-1.8 with different blend compositions (MCPS-1.8/BVPy-34, wt/wt), the samples were heated to and kept at 120°C for 15 min followed by cooling to low temperature at a rate of 1°C/min.

which come much closer compared to the pure components. The most remarkable miscibility enhancement was observed for BVPy-34/MCPS-1.8k blends as shown in Fig. 12. All the blends show only one T_g intermediate between the pure components. As the T_g s of the blends are very close to the calculated value using the Fox equation, $1/T_g = W_1/T_{g1} + W_2/T_{g2}$, it was concluded that to compatibilize BVPy-34 with PS, only one end carboxyl on the PS chain is enough as long as the molar mass of PS is not very high.

3.6. Morphology

The effects of introducing the hydrogen-bonding interaction into the blends on the morphology can be clearly seen in the TEM observations. A striking difference between morphologies of the PVPy/MCPS-1.8 and PVPy/PS-2.3 observed by TEM is shown in Fig. 13. Both blends are phase separated, where the dark regions correspond to the PVPy phase. For PVPy/PS-2.3 (1:2) blends in which no hydrogen bonding exists, the phase separation is very coarse with a domain size of ca. 200–300 nm. In contrast, for the PVPy/MCPS-1.8 (1:2) blends composed of hydrogen-bonding graft copolymers, the phase separation is much finer with a characteristic size smaller than 40 nm. Thus, the hydrogen bonding between the two components plays a substantial role in improving the miscibility.

4. Conclusions

Soluble graft-like complexes were obtained via hydrogen bonding interaction between poly(4-vinyl pyridine) (PVPy) or poly(butyl acrylate-co-4-vinyl pyridine) (BVPy) and mono-carboxy terminated polystyrene (MCPS). In the blend solutions, the grafting of MCPS onto PVPy or BVPy backbones leads to graft-like complexes showing much larger average hydrodynamic radius (R_h) than is

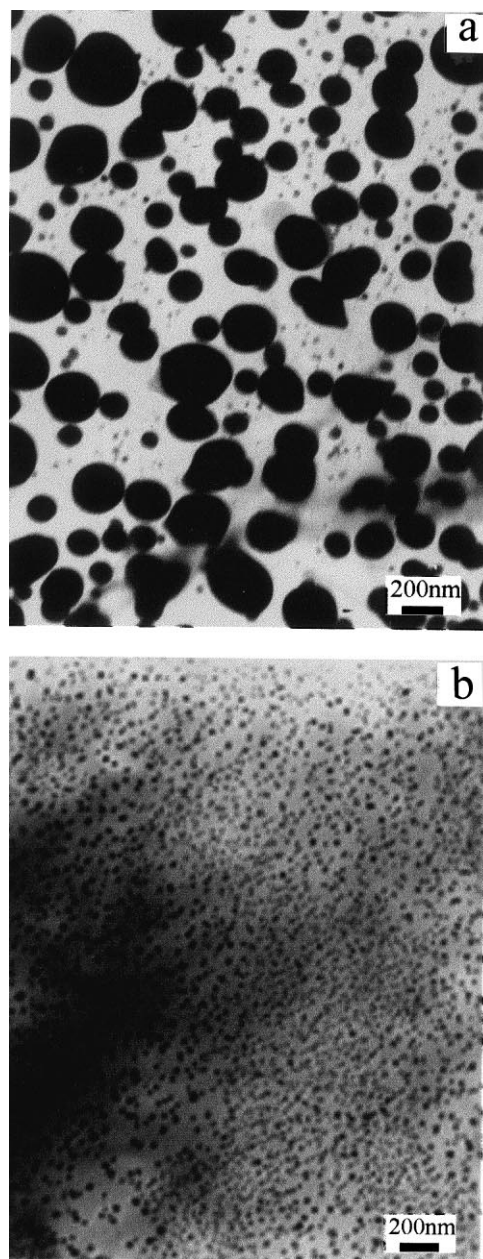


Fig. 13. Transmission electron micrographs of: (a) PVPy/PS-2.3 (1:2) and (b) PVPy/MCPS-1.8 (1:2). All blends were stained with I_2 vapor, and the dark region corresponds to the PVPy-rich phase.

shown by either component alone. Meanwhile, it shows a positive deviation in the viscosity–composition curves compared to that expected by additivity law. Both viscometry and LLS showed a strong effect of molar mass of MCPS on grafting, e.g. the number of branches on each PVPy backbone decreases from 330 to 3 as the molar mass increased from 1.8k to 23.4k. Fluorescence measurements of the energy transfer efficiency between the labeled PVPy coils provided a further support to the “graft-complexation” and its dependence on the molar mass of MCPS. In bulk, DSC results and morphology studies show that although PVPy and MCPS are connected by hydrogen

bonding, two-phase structures in their blends always exist. Besides, thermal history greatly influences the phase behavior and the degree of mixing of the blends which can probably be attributed to the disruption and reorganization of the hydrogen bonding during heating and cooling of the samples. When we decrease the VPy content, e.g. in the blends of MCPS-1.8 and BVPy-34 with much lower T_g , a single-phase structure over the whole composition range is obtained.

Acknowledgements

This work was supported by National Natural Science Foundation of China (NNSFC, nos. 59773023, 29992590), the National Basic Research Project—Macromolecular Condensed State. The LLS experiments were conducted at Dr Wu Chi's laboratory, i.e. the Open Laboratory of Bond-Selective Chemistry, Department of Chemical Physics, University of Science and Technology of China.

References

- [1] Jiang M, Li M, Xiang M, Zhou H. *Adv Polym Sci* 1999;46:121.
- [2] Tsuchida E, Abe K. *Adv Polym Sci* 1982;45:1.
- [3] Zhu L, Jiang M, Liu L, Zhou H, Fan L, Zhang Y. *J Macromol Sci Phys B* 1998;37(6):827.
- [4] Xiang M, Jiang M, Zhang Y, Wu C. *Macromolecules* 1997;30:2313.
- [5] Xiang M, Jiang M, Zhang Y, Wu C, Feng L. *Macromolecules* 1997;30:5339.
- [6] Zhang Y, Xiang M, Jiang M, Wu C. *Macromolecules* 1997;30:2035.
- [7] Zhang Y, Xiang M, Jiang M, Wu C. *Macromolecules* 1997;30:6084.
- [8] Zhu L, Jiang M, Liu L, Zhou H, Fan L, Zhang Y, Zhang Y, Wu C. *J Macromol Sci Phys B* 1998;37(6):805.
- [9] Jiang M, Qiu X, Qin W, Fei L. *Macromolecules* 1995;28:730.
- [10] Qiu X, Jiang M. *Polymer* 1994;35:5084.
- [11] Qiu X, Jiang M. *Polymer* 1995;36:3601.
- [12] Zhou H, Xiang M, Chen W, Jiang M. *Macromol Chem Phys* 1991;198:809.
- [13] Weiss RA, Sasongko S, Jérôme R. *Macromolecules* 1991;24:2271.
- [14] Plante M, Bazuin CG. *Macromolecules* 1997;30:2613.
- [15] Bazuin CG, Plante M, Varshney SK. *Macromolecules* 1997;30:2618.
- [16] Liu S, Zhang G, Jiang M. *Polymer* 1999;40:5449.
- [17] Zhong X, Eisenberg A. *Macromolecules* 1994;27:1751.
- [18] Chu B. *Laser light scattering*. 2nd ed.. New York: Academic Press, 1991.
- [19] Fredrickson GH. *Macromolecules* 1993;26:2825.
- [20] Ikkala O, Ruokolainen J, ten Brinke G, Torkkeli M, Serimaa R. *Macromolecules* 1995;28:7088.